ISSN 1066-3622, Radiochemistry, 2019, Vol. 61, No. 2, pp. 233–237. © Pleiades Publishing, Inc., 2019.

Preclinical Evaluation of ^{99m}Tc-Ethambutol, an Alternative Tuberculosis Diagnostic Tool

S. Q. Shah*[a] and N. Ullah[a]

[a] *Biochemistry Section, Institute of Chemical Sciences, University of Peshawar, Peshawar, 25120 KPK, Pakistan*

**e-mail: ssqaiser2002@yahoo.com*

Received March 1, 2018; revised January 31, 2019; accepted February 4, 2019

Abstract—^{99m}Tc-ethambutol was preclinically evaluated as an alternative diagnostic tuberculosis agent. Its radiochemical purity, stability in saline and serum, in vitro *Mycobacterium tuberculosis* (MBT) binding, and biodistribution in mice were studied, and targeted imaging in model rabbits was performed. The following labeling conditions were found to be optimum: 3 mg of EMB, 150 μg of stannous fluoride, 3 mCi of sodium pertechnetate, pH 5.6. The highest product yield was reached in the time interval 30–90 min after reconstitution. The relative content of ^{99m}Tc-EMB in normal saline at room temperature decreased to 90 ± 0.25% in 240 min. ^{99m}Tc-EMB was stable in vitro in serum at 37°C, with 16.8 ± 0.3% radioimpurities accumulated in 16 h. ^{99m}Tc-EMB showed 69.8 ± 1.5% in vitro uptake in live strains of MBT. High in vivo accumulation (15.5 ± 0.8% ID) of the labeled EMB was observed in the infected site of model mice as compared to the normal and inflamed (muscles) sites. High uptake in the MBT infected site of a model rabbit was seen scintigraphically at 120 min after the intravenous administration of the ^{99m}Tc-EMB. Stability in normal saline and serum, substantial in vitro MBT uptake, high in vivo accumulation in the infected site, and accurate scintigraphy of the infected site make ^{99m}Tc-EMB promising as a novel alternative diagnostic tool for tuberculosis.

Keywords: ethambutol, Mycobacterium tuberculosis, biodistribution, scintigraphy

DOI: 10.1134/S1066362219020176

The diagnosis and treatment of tuberculosis (TB) remain exigent in clinical practice. The gold standards for diagnosis of TB are pathological trials and culture of a specimen taken from the infectious site. However, acquiring a sample is always complicated because the site of TB may be unknown or biopsy may be too insidious [1]. Further, obtaining a sample from the TB suspected site for pathological assessments may also be full of errors leading to false diagnosis. Therefore, diagnosis of TB with imaging techniques is indispensable [2].

Anatomical imaging (AI) with radiological methods assesses structural transformations in tissue architecture in the infectious site. These transformations become visible only in advanced stage of the disease when the tissue damage becomes substantial. Likewise, restitution of the tissue architecture lags behind proper and in-time therapy of infection, posing anatomic imaging erroneous for diagnosis and therapy [3–5].

Molecular imaging (MI) of infection has been the focus of investigators, resulting in the introduction of a wide variety of molecular probes in the clinical or preclinical setting for imaging [6, 7]. MI provides the information regarding the infected site on the basis of metabolic changes, thereby facilitating the clinicians for the in-time diagnosis and treatment of the infection. One could take advantage of MI with the objectives including noninvasive and early diagnosis of infection, differentiation of infection from sterile inflammation, monitoring of response to antimicrobial therapy, prognostication, and identification of the offending agent without the need for the often difficult, time-consuming, and sometimes unsuccessful process required to obtain samples and culture the microbe [8].

Different antimicrobial drugs have been efficiently labeled with various radionuclides and experienced for localizing in vivo infectious sites in a variety of models and humans. Ciprofloxacin was the first ever tested radiolabeled antibacterial agent. Many other antibiotics, including fluoroquinolones, cephalosporins, and antituberculous drugs, have later been successfully labeled and evaluated in preclinical and clinical studies [9–13].

Ethambutol (EMB) [(2*S*,2'*S*)-2,2'-(1,2-ethanediyldiimino)di(1-butanol), see structure below] is an antimycobacterial agent widely used to treat *Mycobacterium tuberculosis*, *Mycobacterium avium complex*, and *Mycobacterium kansasii*. EMB through its bacteriostatic effects blocks DNA and RNA enzymes, thereby inhibiting protein synthesis [14]. According to our knowledge, it was labeled with ^{99m}Tc using hypophosphorous acid as a reducing agent, and its pharmacokinetics was assessed in animals. However, its potential as infection and TB radiotracer was not evaluated [15]. The radiolabeling of EMB with ^{99m}Tc was also studied by another research group using stannous tartrate as a reducing agent and *p*-aminobenzoic acid as a stabilizer. Its clinical efficacy as TB radiotracer was examined in human [16].

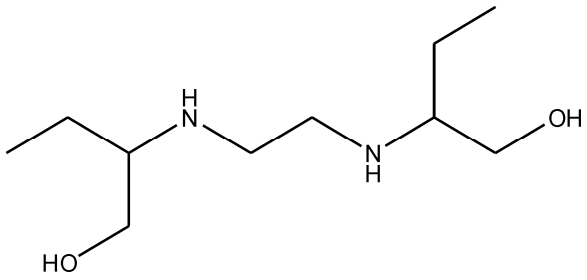

Ethambutol

In this study, we examined the feasibility of labeling EMB with ^{99m}Tc using stannous fluoride as a reducing agent and compared the radiobiological characteristics of ^{99m}Tc-EMB with those of the reported tuberculosis radiopharmaceuticals [17, 18]. The radiochemical purity, stability in saline, in vitro stability in serum, in vitro MBT binding, and biodistribution in model mice were evaluated, and targeted imaging in model rabbits was performed.

EXPERIMENTAL

Materials. Ethambutol (EMB) and all chemicals and solvents were obtained from Merck. HPLC (Shimadzu), well counter (Ludlum), dose calibrator (Capintech), and single photon emission computed tomograph (Nuclearmedizine) were used.

^{99m}Tc-EMB. In five sterilized vials, 1.0 to 5.0 mg (with 1.0 mg step) of EMB was mixed with 50 to 250 μg (with 50 μg step) of stannous fluoride, which was followed by addition of 1.0 to 5.0 mCi (with 1.0 mCi step) of sodium pertechnetate. The pH in each vial was adjusted with 0.01 M HCl to 5.6. The mixture was filtered through a Millipore filter and evaluated for radiochemical purity for up to 4 h at room temperature.

Radiochemical purity. The radiochemical purity of the mixtures was evaluated using TLC with a dual mobile system. An aliquot of freshly prepared ^{99m}Tc-EMB was spotted on a TLC strip (silica gel, Merck). After drying, separate strips were developed in acetone and ethanol–water–ammonia (2 : 5 : 1) mobile systems. The developed strips were measured with a radio-TLC scanner.

HPLC analysis. HPLC analysis was performed using the reported method [17]. Briefly, 10 μL of the labeled EMB solution was injected into the HPLC system, and the mobile phase was fed for 15 min at a flow rate of 1 mL min^{-1}. The activity in various fractions collected at different intervals was measured with a well counter.

In vitro stability in serum of labeled EMB was analyzed by TLC. ^{99m}Tc-EMB (0.3 mL) was mixed with 1.7 mL of fresh serum and incubated at 37°C. Thereafter, 1 μL of the incubated mixture was withdrawn and spotted on a TLC strip, which was developed using acetone and ethanol–ammonia–water (2 : 1 : 5) as solvents and measured with a well counter.

MBT in vitro binding of labeled EMB was determined using the reported method [19]. Briefly, 1.6 mL of live MBT containing about 1×10^8 colony-forming units (CFU) was mixed with 0.2 mCi of labeled EMB and incubated for 60 min at 4°C. After centrifugation for 10 min at 2000 rpm, followed by removal of the supernatant, 0.5 mL of the buffer was added. The activity was measured using a single-well γ-counter interfaced with a scalar count rate meter.

Biodistribution. Healthy mice (weight 20–30 g) were used for determining the biodistribution of ^{99m}Tc-EMB. The mice were divided in two groups (A and B). To all the mice of group A, broth containing 1×10^8 CFU of MBT in 0.1 mL of saline was intramuscularly injected to one thigh, which was followed by the injection of 0.1 mL of turpentine oil to the contralateral thigh. After 12 h, 0.5 mCi (0.1 mL) of labeled EMB was intravenously injected to all the mice of group A. The procedure followed the guidelines of the PNRA and Ethics Committee. The activity per gram of different organs of mice was measured using a well counter. Mice of group B were injected with heat-killed MBT instead of live MBT, and the rest of the

procedure was the same as for group A mice.

In vivo imaging. Healthy rabbits (weight 3.0–4.0 kg) were used for examining the scintigraphic accuracy of the labeled EMB. The rabbits were divided in groups A and B. Rabbits of group A were artificially infected using 0.1 mL (1×10^8 CFU) of MBT broth in saline. After 24 h, 1 mCi (0.2 mL) of labeled EMB was injected intravenously. Then, the animal was scintigraphically examined using a γ-camera at different intervals. The entire procedure was repeated for group B rabbits without inducing the artificial infection. All rabbits were treated in accordance with instructions of the PNRA and ethics committee.

Statistical analysis. The results are expressed as percents of injected dose per gram (% ID/g) or ratios ± SEM. Statistical analysis was performed using the Student's *t*-test.

RESULTS AND DISCUSSION

^{99m}Tc-EMB synthesis and radiochemical purity. The formulation with 3 mg of EMB, 150 μg of stannous fluoride, and 3 mCi of sodium pertechnetate showed the highest radiochemical purity (RCP) in normal saline in the time interval 30–90 min after reconstitution. For the product obtained under these conditions, RCP in normal saline (NS) at room temperature was monitored for a period of up to 240 min; the results were compared to those obtained recently for other tuberculosis radiopharmaceuticals [17, 18] (Fig. 1). The RCP of ^{99m}Tc-EMB in NS at 1, 30, 60, 90, 120, and 240 min was 97.2 ± 0.5, 98.5 ± 0.4, 98.1 ± 0.4, 97.0 ± 0.5, 95.5 ± 0.4, and 92.0 ± 0.5%, respectively. Its stability is similar to that of ^{99m}Tc(CO)$_3$-Rifabutin dithiocarbamate [^{99m}Tc(CO)$_3$-RFND] [17] and ^{99m}Tc-Rifabutin (^{99m}Tc-RFN) [18].

Stability in serum. The in vitro stability of ^{99m}Tc-EMB, ^{99m}Tc(CO)$_3$-RFND [17], and ^{99m}Tc-RFN [18] in serum at 37°C is compared in Fig. 2. The radiochemical purity of ^{99m}Tc-EMB at 0, 2, 4, 6, 8, 10, 12, 14, and 16 h post labeling was 98.5 ± 0.3, 95.3 ± 0.3, 92.1 ± 0.3, 90.0 ± 0.3, 88.5 ± 0.3, 86.9 ± 0.3, 86.5 ± 0.4, 84.7 ± 0.3, and 83.4 ± 0.3%, respectively. The overall decay observed at 37°C in serum in 16 h was 15.10%. The data obtained for ^{99m}Tc(CO)$_3$-RFND [17] and ^{99m}Tc-RFN [18] are similar. The detagging is in the acceptable limit in accordance with the US and British pharmacopoeias.

In vitro MBT binding of ^{99m}Tc-EMB, ^{99m}Tc(CO)$_3$-RFND [17], and ^{99m}Tc-RFN [18] is shown in Fig. 3. The ^{99m}Tc-EMB uptake in live MBT was 25.8 ± 0.5, 56.3 ± 0.6, 74.3 ± 0.6, and 52.5 ± 0.5%, and that in heat-killed MBT, 9.5 ± 1.5, 10.0 ± 1.2, 12.5 ± 1.0, and 10.0 ± 1.4% in 30, 50, 90, and 120 min, respectively. The data obtained for ^{99m}Tc(CO)$_3$-RFND [17] and ^{99m}Tc-RFN [18] are similar.

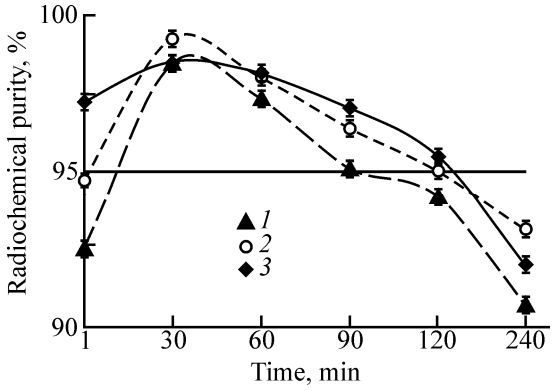

Fig. 1. Comparison of the radiochemical purity of (*1*) ^{99m}Tc-RFN, (*2*) ^{99m}Tc(CO)$_3$-RFND, and (*3*) ^{99m}Tc-EMB in saline.

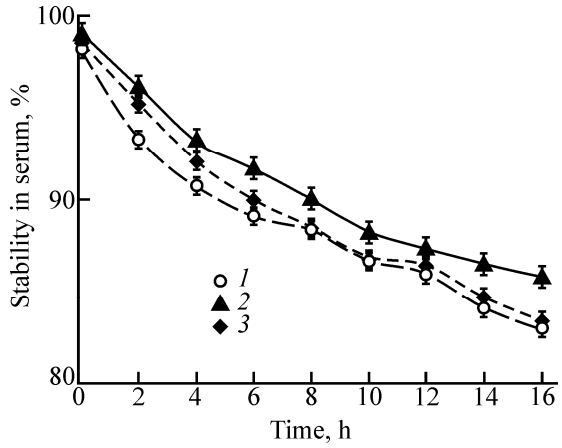

Fig. 2. Comparison of the stability of (*1*) ^{99m}Tc-RFN, (*2*) ^{99m}Tc(CO)$_3$-RFND, and (*3*) ^{99m}Tc-EMB in serum.

Biodistribution of ^{99m}Tc-labeled EMB in various organs of mice infected with live (group A) and heat-killed (group B) MBT is presented in the table. In groups A and B, the uptake of labeled EMB at different intervals (~30 to 120 min) in normal muscle (1 g) remained stable between 2.00 to 3.00% ID/g. Similar stable pattern was observed in the inflamed muscle of both groups of the animals. The distribution of labeled EMB in the infected muscle of group A and B animals

Biodistribution of labelled EMB in mice (% ID/g) at indicated times post injection

Organs, tissues	In live strains				In heat-killed strains			
	30 min	60 min	90 min	120 min	30 min	60 min	90 min	120 min
Infected muscle	4.9 ± 0.5	11.4 ± 0.4	15.0 ± 0.6	10.5 ± 0.5	1.9 ± 0.5	2.0 ± 0.6	2.5 ± 0.4	2.0 ± 0.4
Inflamed muscle	2.5 ± 0.3	3.5 ± 0.4	3.0 ± 0.4	3.0 ± 0.4	2.0 ± 0.5	3.5 ± 0.4	3.0 ± 0.4	3.0 ± 0.4
Normal muscle	2.00 ± 0.25	3.00 ± 0.25	3.0 ± 0.3	2.50 ± 0.20	2.00 ± 0.20	3.0 ± 0.3	3.0 ± 0.4	2.50 ± 0.25
Blood	22.5 ± 0.4	14.6 ± 0.4	10.9 ± 0.3	5.2 ± 0.4	21.6 ± 0.4	15.0 ± 0.5	11.0 ± 0.4	5.0 ± 0.4
Liver	21.9 ± 0.5	12.5 ± 0.5	11.9 ± 0.6	6.5 ± 0.5	20.9 ± 0.5	12.0 ± 0.5	10.3 ± 0.5	6.4 ± 0.6
Spleen	10.6 ± 0.4	9.6 ± 0.4	6.6 ± 0.5	5.0 ± 0.4	10.5 ± 0.5	9.3 ± 0.6	6.4 ± 0.5	5.1 ± 0.5
Kidneys	8.5 ± 0.6	17.8 ± 0.5	19.2 ± 0.5	21.6 ± 0.5	8.3 ± 0.5	17.5 ± 0.5	19.5 ± 0.4	21.8 ± 0.4
Stomach + intestines	10.0 ± 0.5	8.9 ± 0.4	7.5 ± 0.4	4.7 ± 0.4	10.0 ± 0.5	8.9 ± 0.5	8.0 ± 0.5	4.6 ± 0.6

showed a different profile. Initially the ^{99m}Tc-EMB uptake in infected muscle of group A was low, and then it increased from 4.9 ± 0.5 to 15.0 ± 0.6% ID/g at 90 min after of intravenous (IV) injection. Later it decreased to 10.5 ± 0.5% ID/g. However, in group B the radioactivity uptake in the infected muscle was significantly lower and similar to that in the normal and inflamed muscles. The distribution pattern of labeled EMB in the infected, inflamed, and normal muscles of groups A and B was similar to that reported for other labeled drugs in [17, 18].

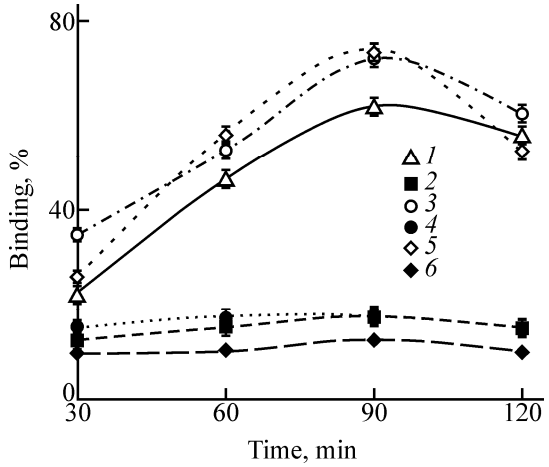

Fig. 3. Comparison of the bacterial uptake of (*1*, *2*) ^{99m}Tc-RFN, (*3*, *4*) ^{99m}Tc(CO)$_3$-RFND, and (*5*, *6*) ^{99m}Tc-EMB in (*1*, *3*, *5*) live and (*2*, *4*, *6*) heat-killed strains of MBT.

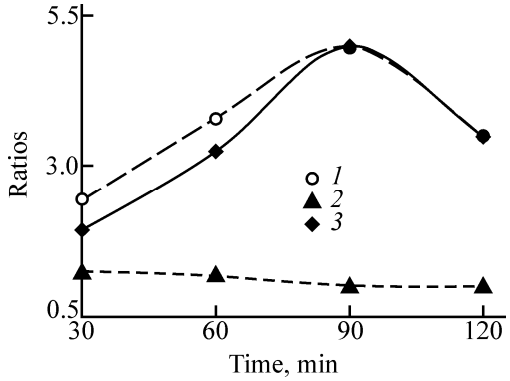

Fig. 4. Uptake ratios for ^{99m}Tc-EMB in mice: (*1*) infected to normal muscle, (*2*) inflamed to normal muscle, and (*3*) infected to inflamed muscle.

The activity uptake in other organs and body fluids was similar in both groups. The uptake in blood, liver, spleen, stomach, and intestine decreased with time, whereas the kidney uptake increased. The pattern was similar to that observed with ^{99m}Tc(CO)$_3$-RFND [17] and ^{99m}Tc-RFN [18].

Figure 4 shows how the uptake ratios in muscles in group A mice vary with time. At 90 min, the activity uptake in the muscle infected with live MBT was almost five time higher than in the normal and inflamed muscles.

In vivo imaging. Figure 5 illustrates the uptake of ^{99m}Tc-EMB in a group A rabbit at different times. The IV injection of ^{99m}Tc-EMB gave better images of various organs of experimental animals as compared to the reported tuberculosis drugs. At 30 min post injection, no significant difference was observed between the infected, inflamed, and normal animals. At 60 min, slightly higher accumulation was observed in the infected part as compared to the normal part. The difference became considerable at 90 min post injection. The uptake of labeled EMB in blood, liver, and spleen was initially high but decreased with time. The kidney images show that, on the contrary, the uptake was initially low and increased with time.

Thus, we have labeled EMB with ^{99m}Tc. The radiochemical purity in normal saline, stability in serum, substantial in vitro MBT uptake, high accumulation in vivo in the infected site, and accurate scintigraphy of the infected site make ^{99m}Tc-EMB promising for the diagnosis of tuberculosis.

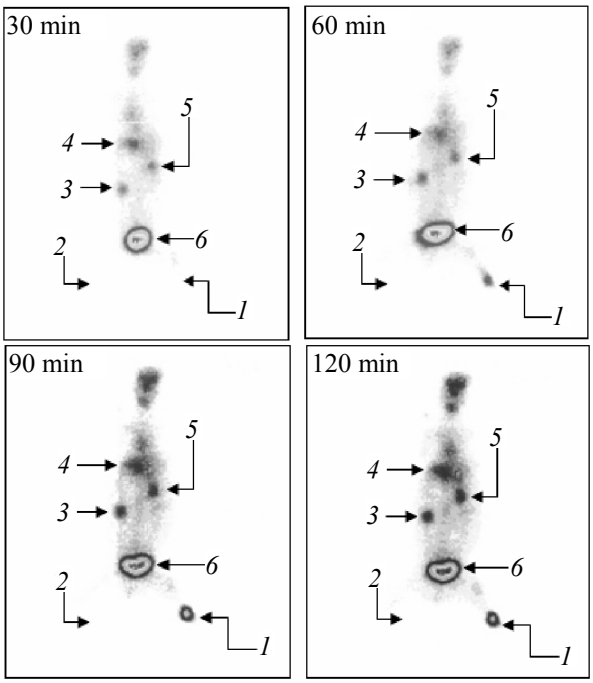

Fig. 5. Whole body imaging of rabbit model. (*1*) Infected muscle, (*2*) inflamed muscle, (*3*) lower kidney, (*4*) heart, (*5*) upper kidney, and (*6*) urinary bladder. The times in which the images were taken are indicated at the images.

CONFLICT OF INTEREST

The authors declare that they have no conflict of interest.

REFERENCES

1. Liu, X., Cheng, D., Gray, B.D., et al., *Nucl. Med. Biol*., 2012, vol. 39, pp. 709–714.
2. Nanni, C., Errani, C., Boriani, L., et al., *J. Nucl. Med*., 2010, vol. 51, pp. 1932–1936.
3. Litzler, P.Y., Manrique, A., Etienne, M., et al., *J. Nucl. Med*., 2010, vol. 51, pp. 1044–1048.
4. Mirbolooki, M.R., Upadhyay, S.K., Constantinescu, C.C., et al., *Nucl. Med. Biol*., 2014, vol. 41, pp. 10–16.
5. Belloli, S., Brioschi, A., Politi, L.S., et al., *Nucl. Med. Biol*., 2013, vol. 40, pp. 831–840.
6. Wang, Y., Chen, L., Liu, X., et al., *Nucl. Med. Biol*., 2013, vol. 40, pp. 89–96.
7. Liu, Z., Wyffels, L., Barber, C., et al., *Nucl. Med. Biol*., 2011, vol. 38, pp. 795–805.
8. Zhang, J., Guo, H., Zhang, S., et al., *Bioorg. Med. Chem. Lett*., 2008, vol. 18, pp. 5168–5170.
9. Chattopadhyay, S., Ghosh, M., Sett, S., et al., *Appl. Radiat. Isot*., 2012, vol. 10, pp. 2384–2387.
10. Roohi, S., Mushtaq, A., Jehangir, M., et al., *J. Radioanal. Nucl. Chem*., 2006, vol. 267, pp. 561–566.
11. Chattopadhyay, S., Das, S.S., Chandra, S., et al. *Appl. Radiat. Isot*., 2010, vol. 68, pp. 314–316.
12. Shah, S.Q., Khan, A.U., and Khan, M.R., *Appl. Radiat. Isot*., 2010, vol. 68, pp. 2255–2560.
13. Shah, S.Q. and Khan, M.R., *J. Radioanal. Nucl. Chem*., 2011, vol. 288, pp. 511–516.
14. Yamada, D., Saiki, S., Furuya, N., et al., *Biochem. Biophys. Commun*., 2016, vol. 471, pp. 109–116.
15. Causse, J.E. et al.,. *Radiat. Appl. Instrum., Part A: Appl. Radiat. Isot*., 1990, vol. 41, pp. 493–496.
16. Singh, N. and Bhatnagar, A., *Tubercul. Res. Treat*., 2010, pp. 1–9.
17. Shah, S.Q. and Momin, S., *J. Glycom. Metab*., 2017, vol. 2, pp. 12–23. DOI: 10.14302/issn.2572-5424.jgm-16-1352.
18. Shah, S.Q. and Alam, M., *Infect. Disord. Drug Targets*, 2017, vol. 3, pp. 185–191. DOI: 10.2174/1871526517666170606114650.
19. Welling, M.M., Annema, A.P., Balter, H.S., et al., *Eur. J. Nucl. Med*., 2000, vol. 27, pp. 292–301.